

CBBN in the CMSSM

Josef Pradler^a and Frank Daniel Steffen

Max-Planck-Institut für Physik, Föhringer Ring 6, D-80805 Munich, Germany

Abstract. Catalyzed big bang nucleosynthesis (CBBN) can lead to an overproduction of ${}^6\text{Li}$ in gravitino dark matter scenarios in which the lighter stau is the lightest Standard Model superpartner. Based on a treatment using the state-of-the-art result for the catalyzed ${}^6\text{Li}$ production cross section, we update the resulting constraint within the framework of the constrained minimal supersymmetric Standard Model (CMSSM). We confront our numerical findings with recently derived conservative limits on the gaugino mass parameter $m_{1/2}$ and the reheating temperature T_R .

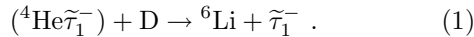
PACS. 12.60.Jv Supersymmetric models – 95.35.+d Dark matter

1 Introduction

Big Bang nucleosynthesis (BBN) is a cornerstone of modern cosmology that allows us to probe physics beyond the Standard Model. It has been realized recently that the presence of massive long-lived negatively charged particles X^- at the time of BBN can have a substantial impact on the primordial light element abundances via bound-state formation [1–11].

In scenarios in which the gravitino \tilde{G} is the lightest supersymmetric particle (LSP), a long-lived X^- may be realized if the lighter stau $\tilde{\tau}_1$ is the next-to-lightest supersymmetric particle (NLSP). In particular, a $\tilde{\tau}_1$ NLSP can be accommodated naturally in the framework of the constrained minimal supersymmetric Standard Model (CMSSM) [12–14, 4, 15] in which the gaugino masses, the scalar masses, and the trilinear scalar couplings are assumed to take on the respective universal values $m_{1/2}$, m_0 , and A_0 at $M_{\text{GUT}} \simeq 2 \times 10^{16}$ GeV. There the stau emerges as the lightest Standard Model superpartner in a large part of the CMSSM parameter space. Since the couplings of the stau to the gravitino are suppressed by the (reduced) Planck scale, $M_{\text{P}} = 2.4 \times 10^{18}$ GeV, $\tilde{\tau}_1$ will typically be long-lived for conserved R-parity¹ and thus $\tilde{\tau}_1^- = X^-$.

Then $\tilde{\tau}_1^-$ and ${}^4\text{He}$ can form bound states, (${}^4\text{He}\tilde{\tau}_1^-$), and too much ${}^6\text{Li}$ can be produced via the catalyzed (CBBN) reaction [1]



This happens at temperatures $T \simeq 10$ keV [1] when standard BBN (SBBN) processes are frozen out. The observationally inferred bound on primordial ${}^6\text{Li}$ then severely restricts the $\tilde{\tau}_1$ abundance at those times² and thereby the $\tilde{\tau}_1$ lifetime $\tau_{\tilde{\tau}_1}$.

^a Speaker; *Email:* jpradler@mppmu.mpg.de

¹ For the case of broken R-parity, see, e.g., [16, 17].

² In this work we assume a standard cosmological history in which $\tilde{\tau}_1$ was in thermal equilibrium before decoupling.

For conserved R-parity, the gravitino LSP is stable and a promising dark matter candidate. After inflation, gravitinos are regenerated [18] in thermal scattering of particles in the primordial plasma. The resulting gravitino density $\Omega_{\tilde{G}}^{\text{TP}}$ will contribute substantially to the dark matter density Ω_{dm} if the radiation-dominated epoch starts with a high reheating temperature T_R [19–21]. In addition, gravitinos are produced in stau NLSP decays with the respective density $\Omega_{\tilde{G}}^{\text{NTP}}$ [22, 12, 23].³

In this work we study gravitino dark matter scenarios within the framework of the CMSSM in which $\tilde{\tau}_1$ is the NLSP. For two exemplary parameter scans, we compute $\Omega_{\tilde{G}} = \Omega_{\tilde{G}}^{\text{TP}} + \Omega_{\tilde{G}}^{\text{NTP}}$ at every point in the associated $(m_0, m_{1/2})$ planes and compare it with Ω_{dm} . The $\tau_{\tilde{\tau}_1}$ -dependent exclusion boundary on the stau abundance from ${}^6\text{Li}$ overproduction allows us to infer the cosmologically disfavored CMSSM region. Our numerical findings are confronted with the recently derived conservative limits on $m_{1/2}$ and T_R [11]. We discuss the present status of the relevant BBN constraints at the end of Sec. 4.

2 Gravitino Dark Matter in the CMSSM

In the CMSSM, the superparticle mass spectrum is determined by specifying m_0 , $m_{1/2}$, A_0 , the ratio of the two MSSM Higgs doublet vacuum expectation values, $\tan\beta$, and the sign of the higgsino mass parameter μ . Then either the lightest neutralino $\tilde{\chi}_1^0$ or the lighter stau $\tilde{\tau}_1$ with respective masses $m_{\tilde{\tau}_1}$ and $m_{\tilde{\chi}_1^0}$ is the lightest Standard Model superpartner and hence the NLSP⁴ whose mass is denoted by m_{NLSP} .

³ We do not include gravitino production from inflaton decays; cf., e.g., [24, 25] and references therein.

⁴ A stop \tilde{t}_1 NLSP is not feasible in the CMSSM [26].

With the gravitino LSP, the relic density from NLSP decays reads

$$\Omega_{\tilde{G}}^{\text{NTP}} h^2 = m_{\tilde{G}} Y_{\text{NLSP}}^{\text{dec}}(T_0) h^2 / \rho_c, \quad (2)$$

where $m_{\tilde{G}}$ is the gravitino mass. The quantity $Y_{\text{NLSP}}^{\text{dec}} = n_{\text{NLSP}}^{\text{dec}}/s$ denotes the NLSP yield where $n_{\text{NLSP}}^{\text{dec}}$ is the number density at decoupling and $s = 2\pi^2 g_* S T^3/45$ the entropy density; $\rho_c/[s(T_0)h^2] = 3.6 \times 10^{-9}$ GeV [27]. We obtain $Y_{\text{NLSP}}^{\text{dec}}$ by employing the computer program `micrOMEGAS 3.17` [28] which we feed with the super-particle mass spectrum computed with `SuSpect 2.34`.⁵

The upper panels in Fig. 1 show contours of $Y_{\text{NLSP}}^{\text{dec}}$ (solid) and m_{NLSP} (dotted) in the $(m_{1/2}, m_0)$ plane for $A_0 = 0$, $\mu > 0$, (a) $\tan\beta = 10$ and (b) $\tan\beta = 30$. Above (below) the dashed line, $m_{\tilde{\chi}_1^0} < m_{\tilde{\tau}_1}$ ($m_{\tilde{\tau}_1} < m_{\tilde{\chi}_1^0}$). The medium gray and the light gray regions at small $m_{1/2}$ are excluded respectively by the mass bounds $m_{\tilde{\chi}_1^\pm} > 94$ GeV and $m_h > 114.4$ GeV from chargino and Higgs searches at LEP [27]. For $\tan\beta = 30$, tachyonic sfermions occur at points in the white corner labeled as ‘‘tachyonic.’’

Let us now explore the parameter space in which the relic gravitino density matches the observed dark matter density [27] $\Omega_{\text{dm}}^{3\sigma} h^2 = 0.105_{-0.030}^{+0.021}$ where h is the Hubble constant in units of $100 \text{ km Mpc}^{-1} \text{ s}^{-1}$. Then, T_R and $m_{\tilde{G}}$ appear in addition to the CMSSM parameters. In the lower panels of Fig. 1, the shaded (green in the web version) bands are the $(m_{1/2}, m_0)$ regions in which

$$0.075 \leq \Omega_{\tilde{G}}^{\text{TP}} h^2 + \Omega_{\tilde{G}}^{\text{NTP}} h^2 \leq 0.126 \quad (3)$$

for the indicated values of T_R and for (c) $m_{\tilde{G}} = m_0$ and (d) $m_{\tilde{G}} = 10$ GeV. For $\Omega_{\tilde{G}}^{\text{TP}}$, we use expression (3) of Ref. [20]⁶ while $\Omega_{\tilde{G}}^{\text{NTP}}$ is computed as explained above. In the dark shaded regions at larger m_0 , the gravitino is not the LSP.

3 Catalyzed BBN of ${}^6\text{Li}$ in the CMSSM

We now focus on the $\tilde{\tau}_1$ NLSP region. For typical values of $Y_{\tilde{\tau}_1}^{\text{dec}} = Y_{\text{NLSP}}^{\text{dec}}/2$ [see Figs. 1 (a,b)], the amount of ${}^6\text{Li}$ produced in the CBBN reaction (1) can be as high as ${}^6\text{Li}/\text{H}|_{\text{CBBN}} = 10^{-7}$ [1,5,11] and hence far in excess of the observationally inferred upper limit on the primordial ${}^6\text{Li}$ abundance [30]

$${}^6\text{Li}/\text{H}|_{\text{obs}} \lesssim 2 \times 10^{-11}. \quad (4)$$

For $\tau_{\tilde{\tau}_1} \lesssim 5 \times 10^3$ s [1,5,6,8,11], however, the staus decay before (1) becomes too efficient so that ${}^6\text{Li}/\text{H}|_{\text{CBBN}}$ can be in agreement with (4). From the $\tau_{\tilde{\tau}_1}$ -dependent upper limit on $Y_{\tilde{\tau}_1}^{\text{dec}}$ computed in [11] by solving the

Boltzmann equations containing the state-of-the-art result for the catalyzed ${}^6\text{Li}$ production cross section [5], we obtain the long-dash-dotted (red in the web version) lines in the lower panels of Fig. 1. The regions to the left of these lines are cosmologically disfavored because of overproduction of ${}^6\text{Li}$.⁷ Note that only the constraint from the primordial D abundance on hadronic energy release [29,31] in $\tilde{\tau}_1$ decays [23,13,32] can be more severe than the one from catalyzed ${}^6\text{Li}$ production [4,33,15,7].⁸ This is shown by the short-dash-dotted (blue in the web version) lines in panel (c) which exclude the region in the $\tilde{\tau}_1$ NLSP region above these lines. In panel (d) the D constraint does not appear; for details see [32,15]. Contours of the NLSP lifetime are shown by the dotted lines.

4 Discussion

The position of the ${}^6\text{Li}$ constraint is governed by the stau lifetime. From the constraint $\tau_{\tilde{\tau}_1} \leq 5 \times 10^3$ s, conservative limits on the gaugino mass parameter,

$$m_{1/2} \geq 0.9 \text{ TeV} \left(\frac{m_{\tilde{G}}}{10 \text{ GeV}} \right)^{2/5}, \quad (5)$$

and the reheating temperature,

$$T_R \leq 4.9 \times 10^7 \text{ GeV} \left(\frac{m_{\tilde{G}}}{10 \text{ GeV}} \right)^{1/5} \quad (6)$$

have been derived recently [11]. Note that these limits, obtained in the framework of the CMSSM, do only depend on $m_{\tilde{G}}$.

The limit (5) emerges since $m_{\tilde{\tau}_1}$ scales with $m_{1/2}$ [see Figs. 1 (a,b)] and since $\tau_{\tilde{\tau}_1}$ is fixed once $m_{\tilde{G}}$ and $m_{\tilde{\tau}_1}$ are specified. The choice $m_{\tilde{G}} = 10$ GeV in Fig. 1 (d) allows for an immediate comparison of our numerical findings with (5) and (6). Only in the vicinity of the dashed line, i.e., in the $\tilde{\tau}_1$ - $\tilde{\chi}_1^0$ coannihilation region, the position of the ${}^6\text{Li}$ constraint approaches its conservative lower limit (5). This is because $\tilde{\tau}_1$ becomes heavier for larger m_0 which shortens $\tau_{\tilde{\tau}_1}$ for fixed $m_{\tilde{G}}$. Contrariwise, the splitting between the actual position of the ${}^6\text{Li}$ constraint and (5) is larger for smaller m_0 . At $m_0 = 10$ GeV, this is more pronounced in Fig. 1 (d) than in Fig. 1 (c). This results from the fact that the increase in $\tan\beta$ leads to a decrease in $m_{\tilde{\tau}_1}$ so that $\tau_{\tilde{\tau}_1}$ becomes larger for fixed $m_{\tilde{G}}$.

The limit (6) relies on thermal gravitino production only, $\Omega_{\tilde{G}}^{\text{TP}} \sim T_R$ [19–21]. Thus the upper limit on T_R can only become more stringent by taking $\Omega_{\tilde{G}}^{\text{NTP}}$ into account. In Fig. 1 (c) we have fixed $m_{\tilde{G}} = m_0$. Thereby, the non-thermal production (2) becomes more important for larger values of m_0 . In addition, $Y_{\tilde{\tau}_1}^{\text{dec}}$ takes on its maximum at a given $m_{1/2}$ in the $\tilde{\tau}_1$ - $\tilde{\chi}_1^0$ coannihilation region. This leads to the bending of the bands (3) towards lower $m_{1/2}$. From Figs. 1 (c,d) we

⁵ We use the following Standard Model parameters: $m_t = 172.5$ GeV, $m_b(m_b)^{\overline{\text{MS}}} = 4.23$ GeV, $\alpha_s^{\overline{\text{MS}}}(m_Z) = 0.1172$, and $\alpha_{\text{em}}^{-1\overline{\text{MS}}}(m_Z) = 127.90896$.

⁶ For the definition of T_R , see Sec. 2 in Ref. [15].

⁷ In this regard, cf. discussion at the end of Sec. 4.

⁸ Additional constraints on the primordial light elements from CBBN can be found in [4,6,7,10].

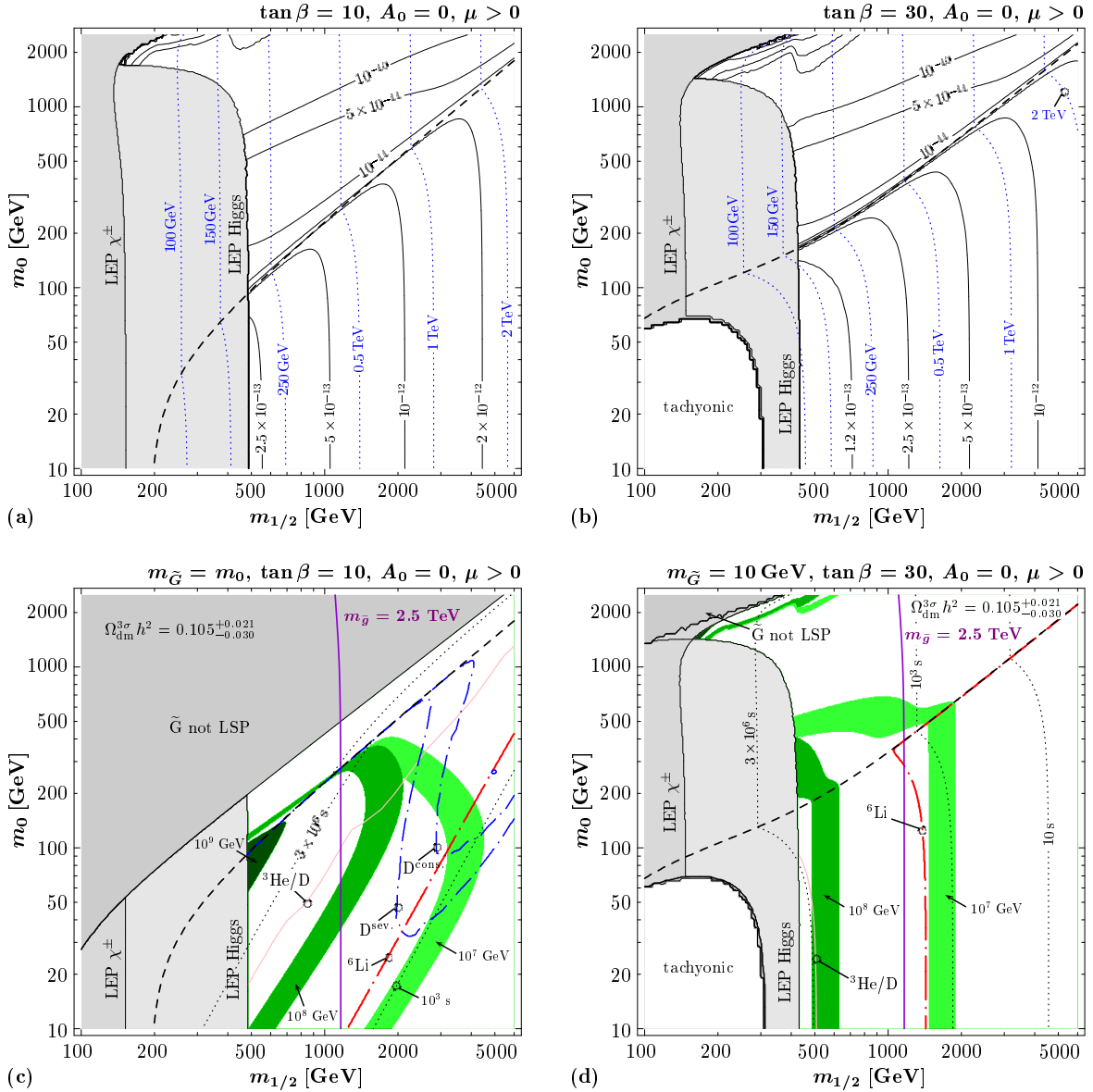


Fig. 1. The $(m_{1/2}, m_0)$ planes for $A_0 = 0$, $\mu > 0$, and the choices (a,c) $\tan \beta = 10$ and (b,d) $\tan \beta = 30$. Above (below) the dashed lines, $m_{\tilde{\chi}_1^0} < m_{\tilde{\tau}_1}$ ($m_{\tilde{\tau}_1} < m_{\tilde{\chi}_1^0}$). The medium gray and the light gray regions at small $m_{1/2}$ are excluded respectively by chargino and Higgs searches at LEP. In the upper panels, contours of Y_{NLSP}^{dec} (solid) and m_{NLSP} (dotted) are shown. In the associated lower panels, we consider scenarios with (c) $m_{\tilde{G}} = m_0$ and (d) $m_{\tilde{G}} = 10$ GeV. The light, medium, and dark shaded (green in the web version) bands indicate the regions in which $0.075 \leq \Omega_{\tilde{G}} h^2 \leq 0.126$ for $T_R = 10^7$, 10^8 , and 10^9 GeV, respectively. In the dark gray region, the gravitino is not the LSP. The dotted lines show contours of the NLSP lifetime. With the $\tilde{\tau}_1$ NLSP, the region to the left of the long-dash-dotted (red in the web version) line is disfavored by the primordial ${}^6\text{Li}$ abundance. Constraints from primordial D disfavor the $\tilde{\tau}_1$ NLSP region above the short-dash-dotted lines. The region to the left of the thin gray (pink in the web version) line is disfavored by ${}^3\text{He}/\text{D}$ [29]. On the solid vertical line (violet in the web version) $m_{\tilde{g}} = 2.5$ TeV.

thus find $T_R \lesssim 10^7$ GeV confirming that (6) indeed provides a good conservative estimate. The bound $T_R \lesssim 10^7$ GeV can be very restrictive for models of inflation and baryogenesis.

Since for a $\tilde{\tau}_1$ NLSP typically $m_0^2 \ll m_{1/2}^2$, it is the gaugino mass parameter $m_{1/2}$ which sets the scale for the low energy superparticle spectrum. Thus, depending on $m_{\tilde{G}}$, the bound (5) implies high values of the superparticle masses which can be associated with a

mass range that will be difficult to probe at the Large Hadron Collider (LHC). This is illustrated by the vertical (violet in the web version) line in Figs. 1 (c,d) which shows the gluino mass contour $m_{\tilde{g}} = 2.5$ TeV.⁹

In the above considerations we have assumed a standard thermal history of the Universe during the radiation-dominated epoch. A substantial entropy re-

⁹ Note that the mass of the lighter stop is $m_{\tilde{t}_1} \simeq 0.7m_{\tilde{g}}$ in the considered $\tilde{\tau}_1$ NLSP regions with $m_h > 114.4$ GeV.

lease after the decoupling of the NLSP but before the onset of BBN may dilute $Y_{\tilde{\tau}_1}^{\text{dec}}$ [34] such that ${}^6\text{Li}/\text{H}|_{\text{CBBN}}$ respects (4) even for $\tau_{\tilde{\tau}_1} \gtrsim 5 \times 10^3 \text{ s}$ [15, 5]. The actual amount of entropy required, however, is model dependent. For example, if entropy is released by an out-of-equilibrium decay of a massive particle species ϕ , the presence of the energy density ρ_ϕ during NLSP decoupling can affect $Y_{\text{NLSP}}^{\text{dec}}$. Furthermore, the branching ratio of the ϕ decays into $\tilde{\tau}_1$ and/or gravitinos may be substantial; see, e.g., [24, 25]. An illustrative scenario taking into account the former effect but neglecting the latter can be found in [15]. As argued in [35], however, a concrete realization of a large entropy release by ϕ decays in the narrow time window after NLSP decoupling and before BBN might be rather difficult to accomplish in the considered scenarios.

Let us finally comment on the present status of BBN constraints on gravitino dark matter scenarios with a long-lived charged slepton NLSP. It has recently been pointed out in Ref. [10] that that bound-state formation of X^- with protons at $T \simeq 1 \text{ keV}$ might well reprocess large fractions of the previously synthesized ${}^6\text{Li}$. The drop in the ${}^6\text{Li}$ abundance at $t \simeq 3 \times 10^6 \text{ s}$ found in [10] is rather drastic. As can be seen from the associated $\tau_{\tilde{\tau}_1}$ contour in Figs. 1 (c,d), this could reopen a ${}^6\text{Li}$ conform window in the collider friendly region of low $m_{\tilde{\tau}_1}$ and low $m_{\tilde{g}}$, provided that the LEP Higgs bound is respected. Unfortunately, at the time of writing, the existing uncertainties in the relevant CBBN nuclear reaction rates in [10] make it difficult to arrive at a final conclusion on ${}^6\text{Li}/\text{H}|_{\text{CBBN}}$ for $\tau_{\tilde{\tau}_1} \gtrsim 3 \times 10^6 \text{ s}$. In this region, however, the ${}^3\text{He}/\text{D}$ constraint on electromagnetic energy release [36] becomes severe and can exclude $\tau_{\tilde{\tau}_1} \gtrsim 10^6 \text{ s}$ [13, 4, 7, 10]. This is illustrated in Figs. 1 (c,d) by the thin gray (pink in the web version) line which is obtained from Fig. 42 of Ref. [29] with $E_{\text{vis}} = 0.3 (m_{\tilde{\tau}_1}^2 - m_{\tilde{G}}^2 + m_{\tilde{\tau}}^2)/2m_{\tilde{\tau}_1}$. Because of the strong sensitivity of the ${}^3\text{He}/\text{D}$ constraint for $10^6 \text{ s} \lesssim \tau_{\tilde{\tau}_1} \lesssim 10^7 \text{ s}$ [29, 31], it still remains difficult to decide whether small cosmologically allowed islands would exist in the CMSSM parameter space for $\tau_{\tilde{\tau}_1} > 5 \times 10^3 \text{ s}$.¹⁰

5 Conclusion

We have considered gravitino dark matter scenarios in which $\tilde{\tau}_1$ is the NLSP. In exemplary CMSSM scenarios we have demonstrated that our recently obtained limit [11] $T_{\text{R}} \leq 4.9 \times 10^7 \text{ GeV} (m_{\tilde{G}}/10 \text{ GeV})^{1/5}$ from catalyzed ${}^6\text{Li}$ production is indeed conservative. In particular, taking into account $\Omega_{\tilde{G}}^{\text{NTP}}$, the T_{R} limit can become considerably more severe. Furthermore, we have shown explicitly that the ${}^6\text{Li}$ constraint can exclude $m_{\tilde{g}} < 2.5 \text{ TeV}$. The cosmologically favored region can thus be associated with a mass range that will be very difficult to probe at the LHC.

¹⁰ With a highly fine-tuned $m_{\tilde{\tau}_1} - m_{\tilde{G}}$ degeneracy leading to $E_{\text{vis}} \rightarrow 0$, any bound on energy release can be evaded.

References

1. M. Pospelov, Phys. Rev. Lett. **98**, 231301 (2007)
2. K. Kohri, F. Takayama, Phys. Rev. **D76**, 063507 (2007)
3. M. Kaplinghat, A. Rajaraman, Phys. Rev. **D74**, 103004 (2006)
4. R.H. Cyburt, J.R. Ellis, B.D. Fields, K.A. Olive, V.C. Spanos, JCAP **0611**, 014 (2006)
5. K. Hamaguchi, T. Hatsuda, M. Kamimura, Y. Kino, T.T. Yanagida, Phys. Lett. **B650**, 268 (2007)
6. C. Bird, K. Koopmans, M. Pospelov (2007), [hep-ph/0703096](#)
7. M. Kawasaki, K. Kohri, T. Moroi, Phys. Lett. **B649**, 436 (2007)
8. F. Takayama (2007), [arXiv:0704.2785 \[hep-ph\]](#)
9. T. Jittoh et al. (2007), [arXiv:0704.2914 \[hep-ph\]](#)
10. K. Jedamzik (2007), [arXiv:0707.2070v1 \[astro-ph\]](#), [arXiv:0707.2070v2 \[astro-ph\]](#)
11. J. Pradler, F.D. Steffen (2007), [arXiv:0710.2213 \[hep-ph\]](#)
12. J.R. Ellis, K.A. Olive, Y. Santoso, V.C. Spanos, Phys. Lett. **B588**, 7 (2004)
13. D.G. Cerdeno, K.Y. Choi, K. Jedamzik, L. Roszkowski, R. Ruiz de Austri, JCAP **0606**, 005 (2006)
14. K. Jedamzik, K.Y. Choi, L. Roszkowski, R. Ruiz de Austri, JCAP **0607**, 007 (2006)
15. J. Pradler, F.D. Steffen, Phys. Lett. **B648**, 224 (2007)
16. W. Buchmüller, L. Covi, K. Hamaguchi, A. Ibarra, T. Yanagida, JHEP **03**, 037 (2007)
17. A. Ibarra (2007), [arXiv:0710.2287 \[hep-ph\]](#)
18. M.Y. Khlopov, A.D. Linde, Phys. Lett. **B138**, 265 (1984)
19. M. Bolz, A. Brandenburg, W. Buchmüller, Nucl. Phys. **B606**, 518 (2001)
20. J. Pradler, F.D. Steffen, Phys. Rev. **D75**, 023509 (2007)
21. V.S. Rychkov, A. Strumia, Phys. Rev. **D75**, 075011 (2007)
22. T. Asaka, K. Hamaguchi, K. Suzuki, Phys. Lett. **B490**, 136 (2000)
23. J.L. Feng, S. Su, F. Takayama, Phys. Rev. **D70**, 075019 (2004)
24. M. Endo, F. Takahashi, T.T. Yanagida (2007), [arXiv:0706.0986 \[hep-ph\]](#)
25. T. Asaka, S. Nakamura, M. Yamaguchi, Phys. Rev. **D74**, 023520 (2006)
26. J.L. Diaz-Cruz, J.R. Ellis, K.A. Olive, Y. Santoso, JHEP **05**, 003 (2007)
27. W.M. Yao et al. (Particle Data Group), J. Phys. **G33**, 1 (2006)
28. G. Belanger, F. Boudjema, A. Pukhov, A. Semenov, Comput. Phys. Commun. **174**, 577 (2006)
29. M. Kawasaki, K. Kohri, T. Moroi, Phys. Rev. **D71**, 083502 (2005)
30. R.H. Cyburt, J.R. Ellis, B.D. Fields, K.A. Olive, Phys. Rev. **D67**, 103521 (2003)
31. K. Jedamzik, Phys. Rev. **D74**, 103509 (2006)
32. F.D. Steffen, JCAP **0609**, 001 (2006)
33. F.D. Steffen, AIP Conf. Proc. **903**, 595 (2007)
34. W. Buchmüller, K. Hamaguchi, M. Ibe, T.T. Yanagida, Phys. Lett. **B643**, 124 (2006)
35. S. Kasuya, F. Takahashi (2007), [arXiv:0709.2634 \[hep-ph\]](#)
36. G. Sigl, K. Jedamzik, D.N. Schramm, V.S. Berezinsky, Phys. Rev. **D52**, 6682 (1995)